Thermoresponsive, recyclable, conductive, and healable polymer nanocomposites with three distinct dynamic bonds

Obed J. Dodo, Leilah Petit, Derrick Dunn, Camryn P. Myers, Dominik Konkolewicz*

Department of Chemistry and Biochemistry, Miami University, 651 E. High Street, Oxford, Ohio 45056, United States

*Corresponding Author: d.konkolewicz@MiamiOH.edu

Abstract

Integration of multiple types of dynamic linkages into one polymer network is challenging and not well understood especially in the design and fabrication of dynamic polymer nanocomposites (DPNs). In this contribution, we present facile methods for synthesizing flexible, healable, conductive, and recyclable thermoresponsive DPNs using three dynamic chemistries playing distinct roles. Dynamic hydrogen bonds accounts for material flexibility and recycling character. Thiol-Michael exchange accounts for thermoresponsive properties. Diels-Alder reaction leads to covalent bonding between polymer matrix and nanocomposite. Overall, presence of multiple types of orthogonal dynamic bonds provided a solution to the trade-off between enhanced mechanical performance and material elongation in DPNs. Efficient reinforcement was achieved using <1 wt.% multiwalled carbon nanotubes as nanocomposite. Resulting DPNs showed excellent healability with over 3 MPa increase in stress compared to unreinforced materials. Due to multiple responsive dynamic linkages, >90% stress relaxation was observed with self-healing achieved within 1 hour of healing time. Increased mechanical strength, electrical conductivity, and re-processability were achieved all while maintaining material flexibility and extensibility, hence highlight the strong promise of these DPNs in the rapidly growing fields of flexible compliant electrodes and strain sensors.

Key words: Dynamic bonds, polymer nanocomposites, electrical conductivity, Diels-Alder, thiol-Michael, hydrogen bonding, thermoresponsive, recyclable.

Introduction

Stimuli responsive and adaptable dynamic polymer materials have attracted significant attention owing to their robust applications in soft pneumatic robots,[1] wearable electronics,[2] energy storage devices,[3] and electronic skins.[4] These "smart" materials respond to biochemical stimuli[5] and physicochemical stimuli such as pH,[6] light,[7] electric field,[8] temperature,[9] and pressure.[10] Dynamic properties in polymer materials can be due to either dynamic covalent bonds or non-covalent interactions.[11] Commonly employed dynamic covalent bonds includes thermo-responsive alkoxyamines,[12] boronic esters,[13] disulfides,[14] oximes,[15] Diels-Alder (DA) linkages,[16] hydrazones,[17] imines,[18] and esters[19] among others. While π–π stacking, hydrogen bonding, and electrostatic interactions are common dynamic non-covalent chemistries useful in the formation of supramolecular polymeric structures.[20] Thermally reversible furan-maleimide DA adducts have received attention since they can be formed under mild conditions, have high chemo-selectivity, and can undergo retro-DA reaction under relatively low temperature of ca. 100 °C.[16] Thiol-Michael (TM) additions are well known for their wide range of functional group tolerance and excellent selectivity among various vinyl groups, making them useful in designing new functional materials.[21] Additionally, dynamic hydrogen bonds have gained popularity in the synthesis of self-healing materials because they are both reversible and weaker than covalent bond, yet stronger than van der Waals bond.[22] Dynamic quadrupole-hydrogen-bond interaction in dimerized 2-ureido-4[1H]-pyrimidinone (UPy) motif is one of the most used hydrogen-bond linkers in dynamic polymer materials,[23] due to its facile synthesis and efficient association.

Despite their potential applications, polymers often have low moduli and limited electrical and magnetic properties, limiting their functionality and performance.[24] To overcome drawbacks associated with homogeneous polymers, various polymer-composites have been explored in literature.[25–27] Reinforced polymer nanocomposites possess superior features such as improved strength, modulus, electrical and thermal properties. Yet, degradation, surface scratches, and mesoscopic damages are major setbacks associated with polymer nanocomposites especially during transport and high-performance applications. However, self-healing polymer nanocomposite materials offers new directions to more sustainable and long-lasting multifunctional materials.[28]

Self-healing mechanisms in polymeric materials can be divided into two categories: extrinsic and intrinsic. Extrinsic self-healing polymers rely on external healing agents such as vascular networks[29] or capsules[30] to facilitate materials recovery, while intrinsic self-healing polymers utilize either dynamic non-covalent[31] or dynamic covalent[32] chemistries. Polymer nanocomposites based on the latter can be referred to as dynamic polymer nanocomposites (DPNs). Nano-reinforcements such as silica, graphene, carbon nanotubes (CNTs), and carbon nanofibers have been utilized in DPNs.[33–35] CNT-based reinforcement gives electrically conductive polymer nanocomposites with enhanced thermal and mechanical characteristics, making CNTs attractive in materials design.[36]

Generally, CNT-based DPNs are made in one of two ways. First is by directly blending CNTs to polymer matrices, leading to mild reinforcements via polymer/CNT non-covalent interaction (e.g., polymer wrapping and polymer absorption). The challenge with this approach is that while CNT structure remains unaltered, transfer of load from polymer to CNT-reinforcement might be low. Second approach involves functionalization of CNT surface (e.g., with amino or carboxyl groups). Even though this approach gives better load transfer, traditional conditions used for CNT modification are very harsh. Functionalizing CNT walls under mild conditions is the best way to fully take advantage of their unique properties. Direct utilization of CNT as a source of dienes or dienophiles in [4+2] DA cycloadditions was first reported by Liu[37] and since then similar chemistry has been reported in nanoscale systems[38,39] but not in bulk materials. Therefore, our group earlier demonstrated an approach for fabricating bulk DPNs using multiwalled carbon nanotubes (MWCNTs) as nano-reinforcements in singly-dynamic DA cross-linked polymeric materials.[40] We showed that well-engineering DPNs from DA bonds between pendant diene groups on polymer chains with π-σ bonds on CNT surface acting as dienophiles can be achieved.

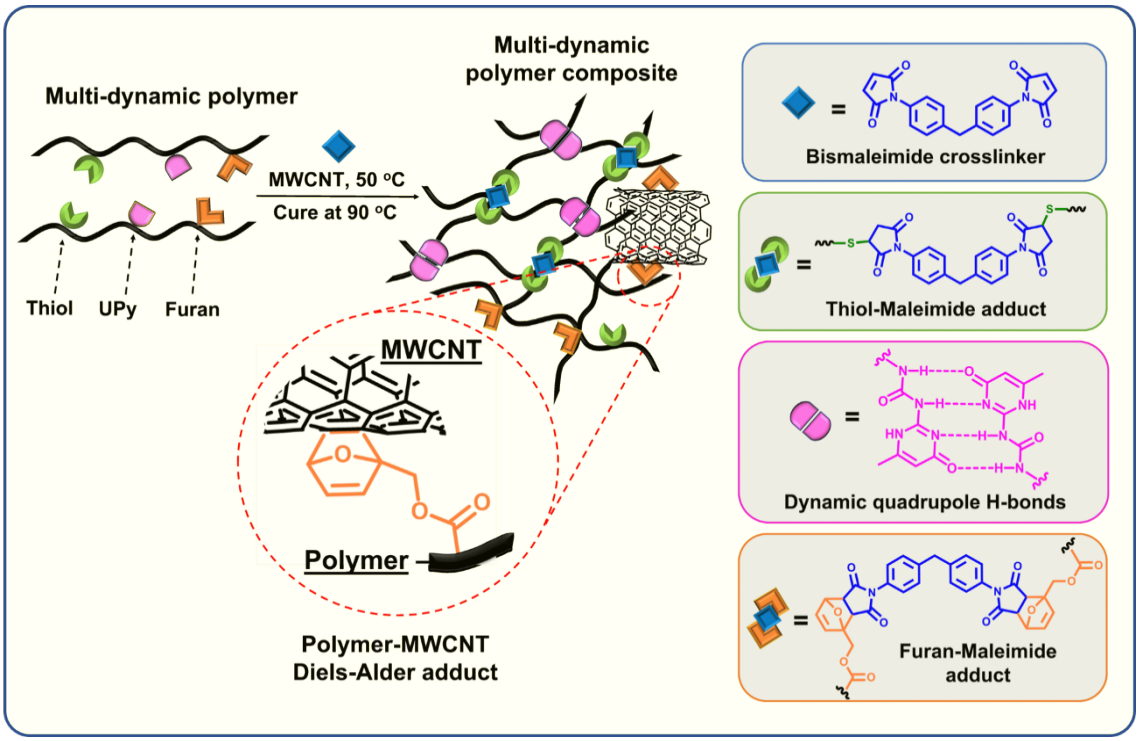

Scheme 1. Reinforcement of a typical triply-dynamic polymer-MWCNT nanocomposite

Herein we demonstrate a facile synthesis of DPNs by utilizing multiple (dual and triply) dynamic networks based on dynamic DA, TM, and quadrupole hydrogen bond chemistries in combination with MWCNT as nanoreinforcement. Multi-dynamic chemistry has been shown to lead to a synergy of each dynamic linker's properties.[41–44] This work presents an approach for fabricating multi-dynamic DPNs with three dynamic chemistries playing distinct dynamic roles. Dynamic hydrogen bonds drive flexibility, reprocessability, and thermoresponsive character. TM exchange facilitates healability, stress relaxation, and thermoresponsive behavior, while DA reaction accounts for effective integration of MWCNT into polymer matrix as illustrated in Scheme 1. Resulting DPNs possess multiple types of orthogonal dynamic linkages and properties such as healability, electrical conductivity, reprocessability, and efficient nanoreinforcement were observed. Increased material strength was observed in reinforced systems while surprisingly maintaining similar strain to the unreinforced material, implying that there was no significant loss in material extensibility despite the integration of MWCNTs. This is unlike most of the previously reported self-healing polymer nanocomposites that give increased strength with a trade-off in decreased elongation, which is the ability of a material to achieve a certain amount of strain.[40,45]

Experimental Section

Synthesis of a typical dual-dynamic poly(EA-UPyMA-FMA) material

Synthesis of poly(EA_{100}-$UPyMA_{3.75}$-$FMA_{3.75}$)

To a 50 mL round bottom flask equipped with a magnetic stir bar, azobisisobutyronitrile (AIBN) (0.02 g, 0.13 mmol), 2-(Propionicacid)yldodecyl trithiocarbonate (PADTC) (0.22 g, 0.63 mmol), , furfuryl-methacrylate (FMA) (0.39 g, 2.36 mmol), 2-ureido-4[1H]-pyrimidinone-methyl-acrylate (UPyMA) (1.00 g, 2.36 mmol), Ethyl acrylate (EA) (6.30 g, 62.89 mmol), and DMF solvent (23 g) were added. The reaction mixture was capped with a rubber septum and placed in an ice bath and stirred for 15 minutes while deoxygenating under nitrogen gas. Then the deoxygenated mixture was transferred to an oil bath and left to stir at 65 °C for 10 hours. Resulting Poly(EA_{100}-$UPyMA_{3.75}$-$FMA_{3.75}$) was confirmed by ^{1}H-NMR indicating 84% conversion and SEC gave a polydispersity Đ of 1.28. The polymer was recovered after precipitating in hexanes and dried in a vacuum oven overnight using a weighed Erlenmeyer flask. After drying under vacuum, the experimental weight of the polymer was obtained and recorded.

Crosslinking a typical poly(EA-UPyMA-FMA) materials by post-polymerization Dynamic Quadrupole Hydrogen Bonding and Diels-Alder Chemistry

Each precursor polymer was combined with (1.5 x polymer weight) amount of DMF. Crosslinking synthesis was performed by dissolving precipitated oven dried polymer in DMF with 0.9 or 0 weight percent of MWCNTs with respect to the polymer weight. To achieve this, the reaction flask containing polymer of known experimental weight and half the total weight amount of DMF required was placed in an ultrasonic bath for one hour until homogenous mixture was obtained. This was followed by an addition of ½ mole equivalent of 1,1′-(methylene-di-4,1-phenyl-ene)bismaleimide (BMI) dissolved in half weight amount of DMF (with respect to polymer weight). The reaction flask was allowed to sonicate for thirty minutes then 0.9 or 0 weight percent amount of MWCNTs was weighed using a weighing boat and added to the reaction flask. The polymer and MWCNTs mixture were allowed to sonicate for ninety minutes so that MWCNTs were dispersed evenly in the polymer matrix. After the MWCNT dispersion, the reaction contents were then transferred into a dog-bone shaped Teflon mold and

covered with a glass cover for 24 hours at 50 °C. Once crosslinked and molded, the dog bone shaped materials were removed from the Teflon mold and allowed to dry in a fume hood for 2 days and overnight in a vacuum oven.

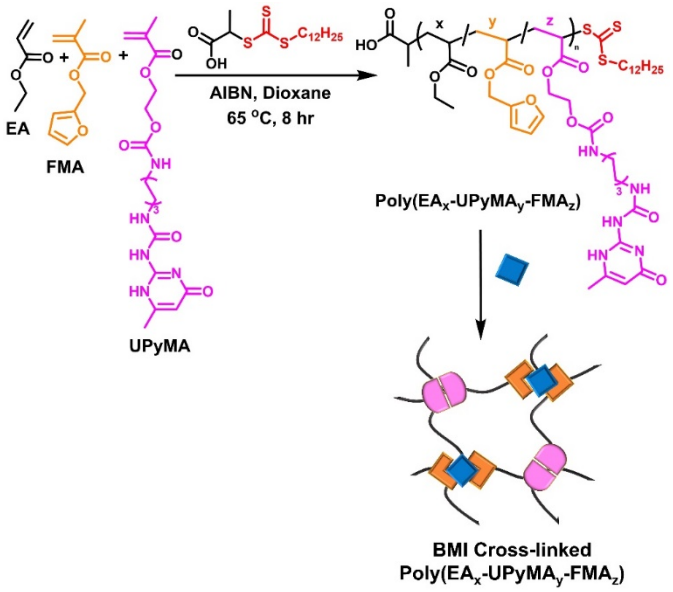

Scheme 2. Typical synthesis of dual-dynamic poly(EA-UPyMA-FMA) materials

Synthesis of a typical dual-dynamic poly(EA-UPyMA-Thiol) material

Synthesis of poly(EA$_{100}$-UPyMA$_{3.75}$-EXEA$_{3.75}$)

To a 50 mL round bottom flask equipped with a magnetic stir bar, AIBN (0.018 g, 0.11 mmol), PADTC (0.25 g, 0.73 mmol), ethyl xanthate ethyl acrylate (EXEA) (0.60 g, 2.73 mmol), UPyMA (1.16 g, 2.73 mmol), EA (7.28 g, 72.70 mmol), and Dioxane (18 g) were added. The reaction mixture was capped with a rubber septum and placed in an ice bath and stirred for 15 minutes while deoxygenating under nitrogen gas. Then the deoxygenated mixture was transferred to an oil bath and left to stir at 65 °C for 16 hours. Resulting Poly(EA$_{100}$-UPyMA$_{3.75}$-EXEA$_{3.75}$) was confirmed by ^{1}H-NMR indicating 98% conversion and SEC gave a Đ of 1.16. The polymer was recovered after precipitating in hexanes and dried in a vacuum oven overnight using a weighed Erlenmeyer flask. After drying under vacuum, the experimental weight of the polymer was obtained and recorded.

General procedure for post polymerization deprotection of EXEA moiety to give poly(EA_{100}-$UPyMA_{3.75}$-$Thiol_{3.75}$)

In a 25 ml round-bottom flask equipped with a magnetic stir bar, the precursor Poly(EA_{100}-$UPyMA_{3.75}$-$EXEA_{3.75}$) was dissolved in 2 equivalents (by weight of polymer) of tetrahydrofuran by sonication. To the mixture, 5 equivalents (by moles, with respect to total moles of PADTC and EXEA) of isopropyl amine were added. The reaction flask was then capped with a rubber septum and deoxygenated with nitrogen for 20 minutes. Then catalytic 0.035 equivalents (by moles, with respect to total moles of PADTC and EXEA) of tributyl phosphine was added to the reaction mixture under nitrogen using a micro syringe and further allowed to deoxygenate for 15 minutes. The reaction was then stirred at room temperature for 24 hrs. The resultant deprotected poly(EA_{100}-$UPyMA_{3.75}$-$Thiol_{3.75}$) was recovered after precipitating in hexanes using a 125 mL Erlenmeyer flask.

Crosslinking dual-dynamic poly(EA_{100}-$UPyMA_{3.75}$-$Thiol_{3.75}$) by Dynamic Quadrupole Hydrogen Bonding and Thiol-Michael Chemistry

In a 125 mL Erlenmeyer flask, deprotected thiol polymer (poly(EA_{100}-$UPyMA_{3.75}$-$Thiol_{3.75}$)) was mixed with 1.5 equivalents (by weight of deprotected polymer) of DMF. In a separate vial, 0.5 equivalents (by moles, with respect to Thiol monomer and PADTC used in the polymer synthesis) of BMI crosslinker was dissolved in 0.5 equivalents (by weight of deprotected polymer) of DMF. The flask and the vial were then placed in an ultrasonic bath until the contents were fully dissolved. Once dissolved, the content in the vial (crosslinker) was added to the flask containing polymer and placed in the ultrasonic bath for few minutes to obtain a homogeneous mixture. Then 0.9 or 0 weight percent amount of MWCNTs was weighed using a weighing boat and added to the reaction flask. The polymer and MWCNTs mixture were allowed to sonicate until MWCNTs were dispersed evenly in the polymer matrix. After the MWCNT dispersion, the reaction contents were then quickly transferred into a dog-bone shaped Teflon mold and covered with a glass cover for 48 hours at 50 °C. Once crosslinked and molded, the dog bone shaped materials were removed from the Teflon mold and allowed to dry in a fume hood for 2 days and overnight in a vacuum oven.

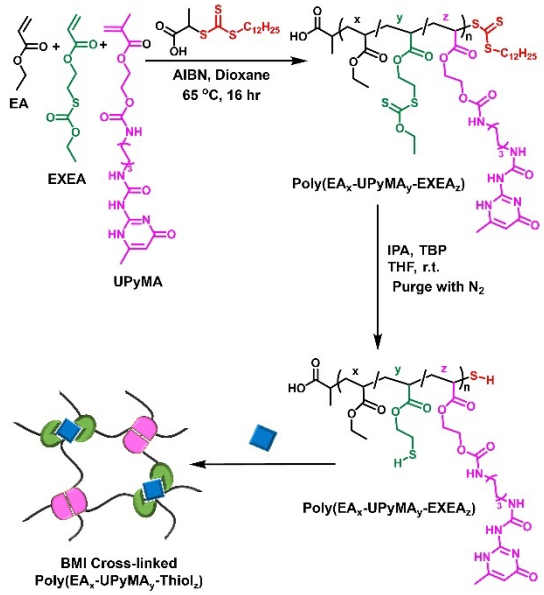

Scheme 3. Typical synthesis of dual-dynamic poly(EA_{100}-$UPyMA_{3.75}$-$Thiol_{3.75}$) materials

Synthesis of a typical triply-dynamic poly(EA-UPyMA-Thiol-FMA) material

Synthesis of poly(EA_{150}-$UPyMA_{3.75}$-$EXEA_{3.75}$-$FMA_{3.75}$)

To a 50 mL round bottom flask equipped with a magnetic stir bar, AIBN (0.01 g, 0.06 mmol), PADTC (0.21 g, 0.61 mmol), FMA (0.38 g, 2.27mmol), EXEA (0.50 g, 2.27 mmol), UPyMA (0.96 g, 2.27 mmol), EA (9.10 g, 90.91 mmol), and Dioxane (23 g) were added. The reaction mixture was capped with a rubber septum and placed in an ice bath and stirred for 15 minutes while deoxygenating under nitrogen gas. Then the deoxygenated mixture was transferred to an oil bath and left to stir at 65 °C for 10 hours. Resulting Poly(EA_{150}-$UPyMA_{3.75}$-$EXEA_{3.75}$-$FMA_{3.75}$) was confirmed by ^{1}H-NMR indicating 79% conversion and SEC gave a Đ of 1.24. The polymer was recovered after precipitating in hexanes and dried in a vacuum oven overnight using a weighed Erlenmeyer flask. After drying under vacuum, the experimental weight of the polymer was obtained and recorded.

General procedure for post polymerization deprotection of EXEA moiety to give poly(EA-UPyMA-Thiol-FMA) materials

In a 25 ml round-bottom flask equipped with a magnetic stir bar, the precursor Poly(EA-UPyMA-EXEA-FMA) material was dissolved in 2 equivalents (by weight of polymer) of tetrahydrofuran by sonication. To the mixture, 5 equivalents (by moles, with respect to total moles of PADTC and EXEA) of isopropyl amine were added. The reaction flask was then capped with a rubber septum and deoxygenated with nitrogen for 20 minutes. Then catalytic 0.035 equivalents (by moles, with respect to total moles of PADTC and EXEA) of tributyl

phosphine was added to the reaction mixture under nitrogen using a micro syringe and further allowed to deoxygenate for 15 minutes. The reaction was then stirred at room temperature for 24 hrs. The resultant deprotected Poly(EA-UPyMA-Thiol-FMA) was recovered after precipitating in hexanes using a 125 mL Erlenmeyer flask.

Crosslinking Triple-dynamic poly(EA-UPyMA-Thiol-FMA) materials by Dynamic Quadrupole Hydrogen Bonding, Thiol-Michael, and Diels-Alder Chemistries

In a 125 mL Erlenmeyer flask, deprotected thiol polymer (Poly(EA-UPyMA-Thiol-FMA)) was mixed with 1.5 equivalents (by weight of deprotected polymer) of DMF. In a separate vial, 0.5 equivalents (by moles, with respect to Thiol monomer and PADTC used in the polymer synthesis) of BMI crosslinker was dissolved in 0.5 equivalents (by weight of deprotected polymer) of DMF. The flask and the vial were then placed in an ultrasonic bath until the contents were fully dissolved. Once dissolved, the content in the vial (crosslinker) was added to the flask containing polymer and placed in the ultrasonic bath for few minutes to obtain a homogeneous mixture. Then 0.9 or 0 weight percent amount of MWCNTs was weighed using a weighing boat and added to the reaction flask. The polymer and MWCNTs mixture were allowed to sonicate until MWCNTs were dispersed evenly in the polymer matrix. After the MWCNT dispersion, the reaction contents were then quickly transferred into a dog-bone shaped Teflon mold and covered with a glass cover for 24 hours at 50 °C and followed by 24 hours at 90 °C. Once crosslinked and molded, the dog bone shaped materials were removed from the Teflon mold and allowed to dry in a fume hood for 2 days and overnight in a vacuum oven.

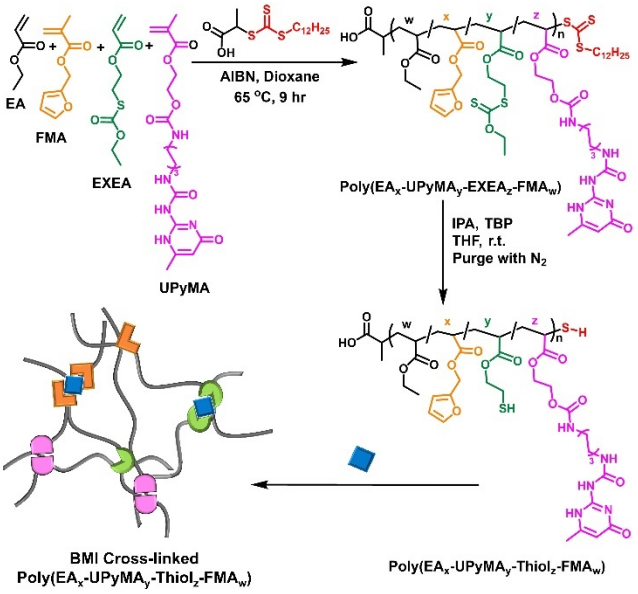

Scheme 4. Typical synthesis of triply-dynamic poly(EA-UPyMA-Thiol-FMA) materials

Procedure for healing experiment

A pristine polymer sample was sliced into two as illustrated in Figure 1 using a razor blade. The cut samples were then placed in close proximity such that their fractured ends were in contact. A little pressure was applied (red arrows in Figure 1) to further ensure that cut samples stayed in contact. Next, both pristine (uncut) and cut samples were heated at 90 °C to ensure that uncut and healed polymer samples were treated similarly for fair comparison.

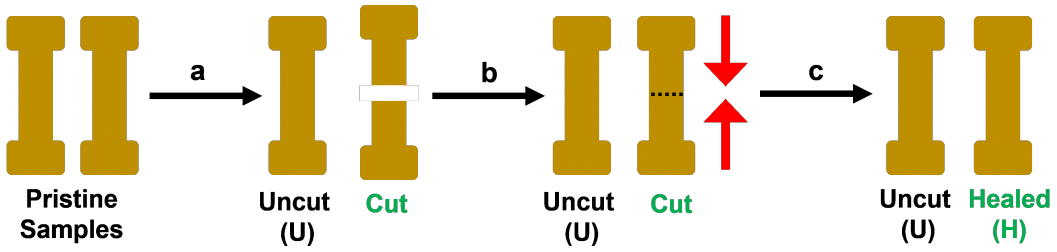

Figure 1. Demonstration of a typical healing experiment used in this study. (a) A pristine sample was sliced using a razor blade. (b) Fractured ends of cut samples were placed back together (c) Pressure was applied to ensure fractured ends of cut samples were in contact and 90 °C was applied for 10 hours.

Results and Discussion

In this study, six different DPNs were synthesized by creating well-defined multi-dynamic polymers using reversible addition-fragmentation chain transfer (RAFT) polymerization[46] (Table S1). Materials in this study were investigated based on varied polymer composition, cross-link density, and degree of polymerization. Moieties responsible for dynamic linkages included 2-ureido-4[1H]-pyrimidinone-methyl-acrylate (UPyMA) capable of exchanging H-bond linkages under ambient and elevated temperatures, FMA and ethyl xanthate ethyl acrylate (EXEA) capable of forming dynamic thermo-responsive DA and Thiol-Maleimide (TM) adducts respectively. Ethyl acrylate (EA) was used as monomer for the backbone of polymers studied, resulting in flexible materials with glass transition temperatures T_g below room temperature (range –5 to +8 °C °C) hence supporting dynamic properties[47,48] (Table 1). Materials synthesized are categorized into three groups of polymers. First group was dual-dynamic with UPyMA and FMA linkers at either 5 mol% crosslinker (poly(EA_{100}-$UPyMA_{2.5}$-$FMA_{2.5}$)) or 7.5 mol% crosslinker (poly(EA_{100}-$UPyMA_{3.75}$-$FMA_{3.75}$)). The second group was dual-dynamic containing UPyMA and Thiol-based crosslinkers at 7.5 mol% linker (poly(EA_{100}-$UPyMA_{3.75}$-$Thiol_{3.75}$)). Third group was triply

dynamic with UPyMA, FMA, and Thiol linkers with a total crosslink density of 7.5 mol%. The triply dynamic materials had three distinct chain lengths of ~100 units (poly(EA_{100}-$UPyMA_{2.5}$-$Thiol_{2.5}$-$FMA_{2.5}$)), ~150 units (poly(EA_{150}-$UPyMA_{3.75}$-$Thiol_{3.75}$-$FMA_{3.75}$)), and ~200 units (poly(EA_{200}-$UPyMA_{5}$-$Thiol_{5}$-FMA_{5})). Scheme S1 provides a flowchart for all materials studied and summarized procedures for all synthesis described in Schemes 2-4. DPNs reinforced with 0.9 wt.% MWCNT were studied in comparison to their pristine polymers with 0 wt.% MWCNT which were used as controls (Table 1). All polymer composition and Đ (1.21 – 1.41) are provided in Table S1. EXEA was employed as a protected thiol monomer and subject to post-polymerization deprotection to obtain free thiol groups (Scheme 3-4). All polydispersity data were collected prior to deprotection (Figure S5). Experimental methods for material characterization are provided in the supporting information.

Table 1. Table outlining all synthesized single-network materials, DSC, and tensile stress-strain data.

Polymer material	**Wt.% CNT**	**T_g (°C)**	**σ_{peak} (MPa)**	**ε_{break} (mm/mm)**	**Y (MPa)**	**Φ (MPa)**
poly(EA_{100}-$UPyMA_{2.50}$-$FMA_{2.50}$)	0	– 1	1.14 ± 0.01	1.70 ± 0.04	1.26 ± 0.05	1.03 ± 0.01
poly(EA_{100}-$UPyMA_{2.50}$-$FMA_{2.50}$)	0.9	– 2	3.2 ± 0.4	1.09 ± 0.07	4.8 ± 0.5	2.37 ± 0.01
poly(EA_{100}-$UPyMA_{3.75}$-$FMA_{3.75}$)	0	0	4.3 ± 0.4	1.12 ± 0.09	6.0 ± 0.3	3.09 ± 0.04
poly(EA_{100}-$UPyMA_{3.75}$-$FMA_{3.75}$)	0.9	0	6.8 ± 0.2	1.0 ± 0.1	11 ± 1	4.23 ± 0.01
poly(EA_{100}-$UPyMA_{3.75}$-$Thiol_{3.75}$)	0	7	2.3 ± 0.2	1.7 ± 0.1	2.27 ± 0.08	2.59 ± 0.09
poly(EA_{100}-$UPyMA_{3.75}$-$Thiol_{3.75}$)	0.9	8	3.8 ± 0.2	0.7 ± 0.1	8 ± 1	1.84 ± 0.01
poly(EA_{100}-$UPyMA_{2.50}$-$Thiol_{2.50}$-$FMA_{2.50}$)	0	0	2.32 ± 0.07	2.47 ± 0.07	1.90 ± 0.03	3.62 ± 0.04
poly(EA_{100}-$UPyMA_{2.50}$-$Thiol_{2.50}$-$FMA_{2.50}$)	0.9	2	4.1 ± 0.3	2.2 ± 0.2	3.81 ± 0.09	4.43 ± 0.01
poly(EA_{150}-$UPyMA_{3.75}$-$Thiol_{3.75}$-$FMA_{3.75}$)	0	– 5	3.1 ± 0.2	1.73 ± 0.08	2.41 ± 0.02	3.82 ± 0.05
poly(EA_{150}-$UPyMA_{3.75}$-$Thiol_{3.75}$-$FMA_{3.75}$)	0.9	0	5.1 ± 0.5	1.2 ± 0.1	7 ± 1	4.3 ± 0.2
poly(EA_{200}-$UPyMA_{5}$-$Thiol_{5}$-FMA_{5})	0	1	4.1 ± 0.5	1.66 ± 0.09	3.07 ± 0.05	4.67 ± 0.04
poly(EA_{200}-$UPyMA_{5}$-$Thiol_{5}$-FMA_{5})	0.9	1	7.3 ± 0.5	1.5 ± 0.2	7.5 ± 0.4	6.70 ± 0.02

The use of methacrylic FMA and UPyMA monomers with acrylic backbone forming monomers could lead to some gradient character, as the methacrylate should incorporate preferentially. Literature reports from Marin et al. revealed a strong correlation between polydispersity and gradient distribution of comonomers in copolymers made using controlled radical polymerization.[49] Hence the distribution of functional monomers in our systems are expected to be relatively non-uniform considering polydispersity values in the range of 1.21 – 1.41 in this study. However, since multiple cross-linking points are available on a single network polymer, the distribution of monomers would have a smaller effect on overall cross-linking efficiency.

Post-polymerization cross-linking of dual-dynamic poly(EA_{100}-$UPyMA_{2.5}$-$FMA_{2.5}$) and poly(EA_{100}-$UPyMA_{3.75}$-$FMA_{3.75}$) (Scheme 2) was achieved via dynamic hydrogen bonds from UPy groups and by using stoichiometric amounts of BMI to cross-link furan groups from FMA via furan-maleimide adduct formation. FMA introduces dienes needed for dynamic covalent DA chemistry in the presence of a maleimide. Since commercially available BMI is 95% pure,[50] using stoichiometric amounts as cross-linker implies that there would be unreacted furan groups available for DA chemistry with MWCNT surface (Scheme 1). For dual-dynamic poly(EA_{100}-$UPyMA_{3.75}$-$Thiol_{3.75}$), dynamic TM addition between Thiol groups and BMI resulted in the cross-linked polymer by formation of TM adduct. (Scheme 3).

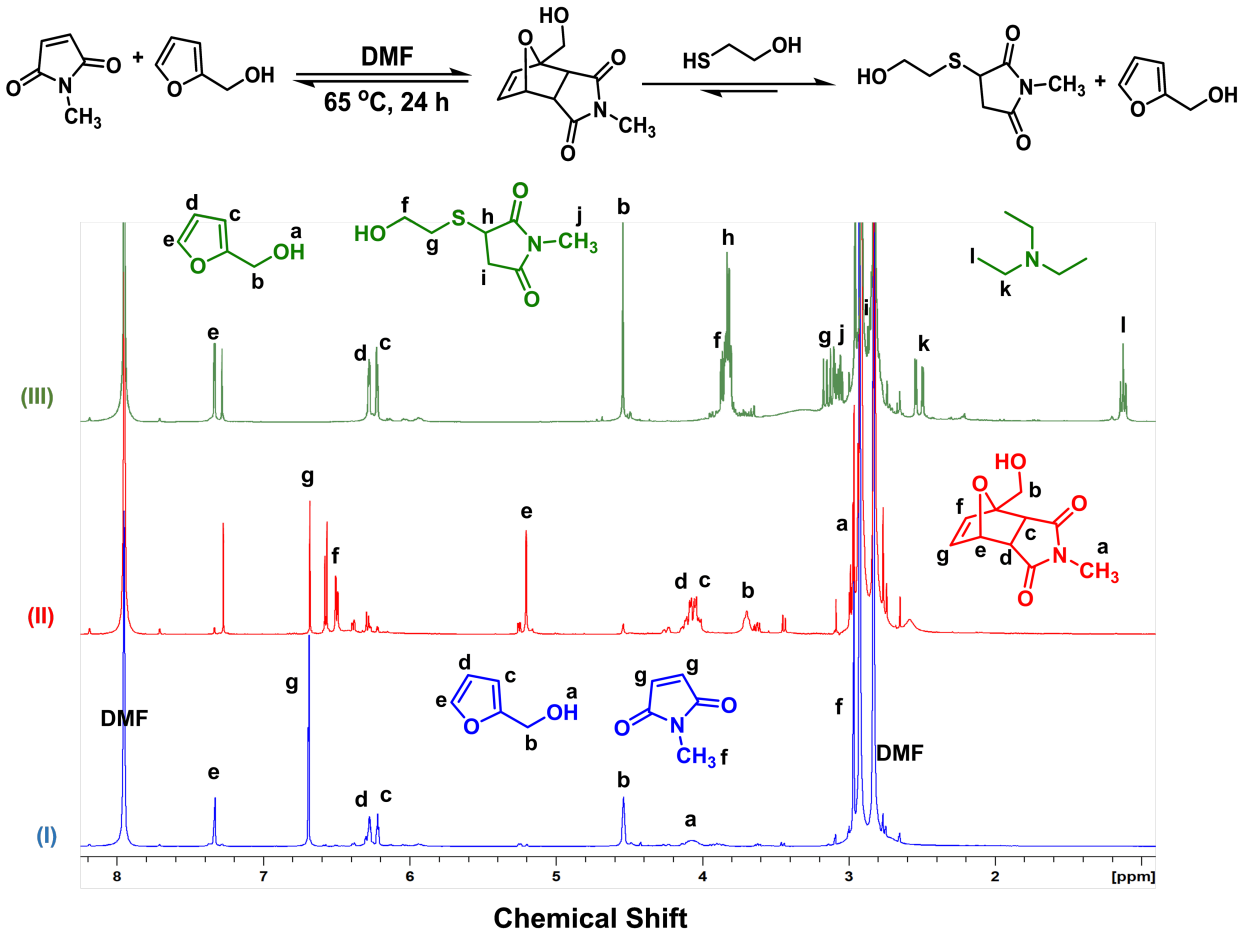

Figure 2. In situ formed DA adduct readily converted to TM adduct in the presence of 2-Mercaptoethan-1-ol. (i) ^{1}H NMR spectrum of a stoichiometric reaction mixture of (Furan-2-yl)methanol and N-methylmaleimide in $CDCl_3$ after mixing. (ii) After heating for 24 hours at 65 ºC shows evidence of DA adduct. And (iii) Introducing stoichiometric amount of ME and catalytic amount of (Triethyl)amine favors formation of corresponding Thiol-Michael adduct after heating for 24 hours at 90 °C.

Before synthesizing the triply dynamic network systems, small molecule studies were performed to evaluate whether the thiol or the furan diene preferentially reacts with the maleimide group, since both pendant furan and thiol groups can react with BMI. Small molecule studies were performed by reacting N-methylmaleimide and furfuryl alcohol (FA) to form a DA adduct which was subjected to dynamic exchange in the presence of 1 equivalent of 2-mercaptoethan-1-ol at 90 °C for 24 hours (Figure 2), see experimental details in supporting information. Interestingly, free FA and the corresponding TM adduct of 2-mercaptoethan-1-ol and N-methylmaleimide were

formed, suggesting that equilibrium strongly favors formation of TM adduct over DA adduct. This transformation occurs by retro-DA reaction of the DA adduct followed by TM addition of 2-mercaptoethan-1-ol to N-methylmaleimide. To confirm this, stoichiometric amount of FA was added to in situ formed TM adduct and after thermal activation of dynamic TM adduct, it was found that FA had no effect on TM adduct as shown in Figure S1. Furthermore, Figure S2 confirms that excess FA had no impact on DA adduct subjected to retro-DA reaction.

These findings show that TM adduct forms preferentially over DA adduct, thus enabling well-engineered triply-dynamic polymer composites from polymers containing UPy, furan, and thiol groups. Cross-linking triply-dynamic materials can be achieved using stoichiometric BMI amount required to cross-link thiol groups via TM adduct, leaving FMA groups to bind to MWCNTs. During synthesis, some FMA furan groups may also react with BMI, therefore DPNs from this study were subjected to a post cross-linking curing process at 90 °C for 24 hours. The rationale is that during the curing process, all possible DA adducts between BMI and furan groups will undergo retro-DA reaction, leading to formation of the more favored TM adduct between BMI and thiol groups. This allows free furan groups to only undergo DA reactions with MWCNT surface via furan dienes on polymer chains and π-bonds on MWCNT surface acting as dienophiles.[37] Hence, all possible chemistries have been illustrated in Scheme 1.

Characterization of materials were carried out using dynamic mechanical analysis (DMA), differential scanning calorimetry (DSC), thermogravimetric analysis (TGA), and tensile testing. Images of typical materials obtained in this study are shown in Figure S3. Thermal degradation profiles of all materials were similar (Figures S6a-c) with degradation occurring in the range 340–360 ^{o}C due to poly(EA) backbone of each material. A typical DSC curve is shown in Figure S6d. Infrared (IR) spectroscopy was used to analyze DP100 triple-dynamic poly(EA_{100}-$UPyMA_{2.5}$-$Thiol_{2.5}$-$FMA_{2.5}$) material with 0 wt.% CNT and 0.9 wt.% CNT in order to identify possible absorption peaks that show evidence of DA adduct. Ideally, stronger absorption peaks representing DA adduct formation between polymer chains and CNT surface are expected to be in 1651 cm^{-1} region. However, identifying and assigning that specific peak in our system is challenging considering that <1 wt.% CNT loading was used. Yet, we observed slightly stronger absorption in the 1600 – 1500 cm^{-1} region for the material containing 0.9 wt.% CNT (Figure S7). This is likely due to the addition of π-bond functionalities from CNTs.

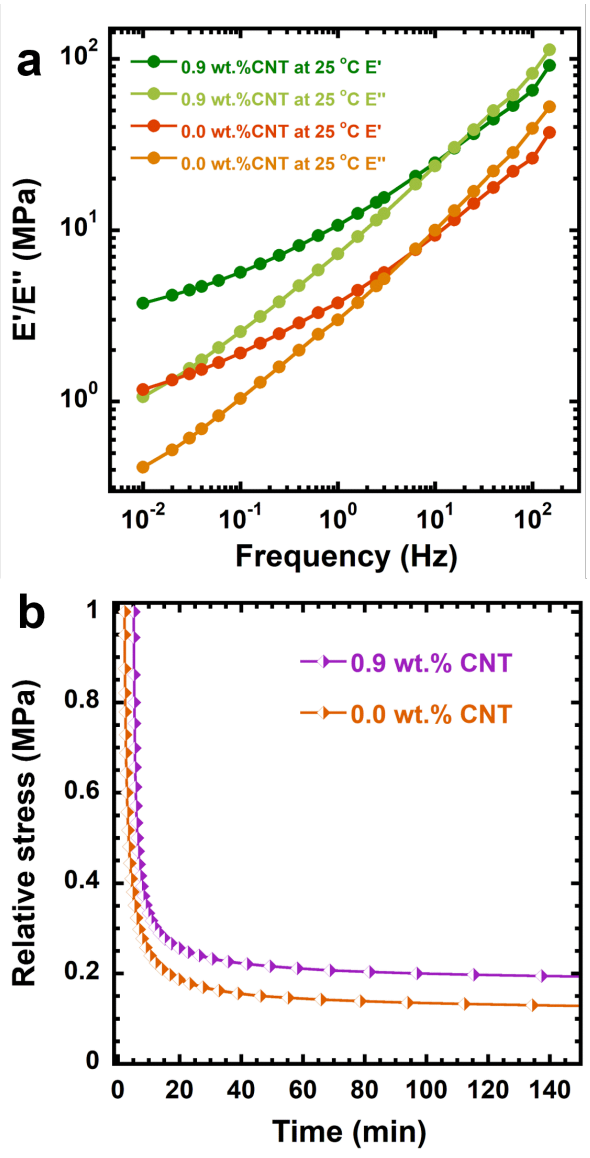

Figure 3. (a) Frequency sweeps of reinforced and unreinforced triply-dynamic poly(EA_{150}-$UPyMA_{3.75}$-$FMA_{3.75}$-$Thiol_{3.75}$) carried out at 25 °C using 0.3% strain. (b) Stress relaxation of reinforced and unreinforced triply-dynamic poly(EA_{150}-$UPyMA_{3.75}$-$FMA_{3.75}$-$Thiol_{3.75}$), relative to the peak stress, carried out at 30 °C using 10% strain.

Several literature reports[51] including findings from Feldman et al.[52] and Leibler et al.[53] confirms that dynamic hydrogen bonds contribute to macroscopic properties such as thermoresponsive behavior, recyclability, and flexibility in dynamic polymer materials respectively. Dynamic TM exchange can also account for thermoresponsive properties, self-healing, malleability, and reprocessability.[54–56] Additionally, DA reaction facilitates effective

reinforcement between functional furan side chains in this study and MWCNT by formation of DA adduct between MWCNT and polymer chains.[37,40] Integration of multiple types of dynamic bonds in polymer materials to synergistically harness their unique properties is rare and not well understood, especially the integration of more than two different orthogonal dynamic exchanges.[57] Hence, DPNs proposed in this study show distinctive dynamic properties that can be attributed to the unique contributions of each dynamic exchange employed.

Initially, impact of MWCNT loading on multi-dynamic materials was determined by looking at both frequency sweep and stress-relaxation of poly(EA_{150}-$UPyMA_{3.75}$-$FMA_{3.75}$-$Thiol_{3.75}$). As seen in Figure 3a, integration of just 0.9 wt.% MWCNTs increases storage modulus of materials by a factor of ~4. At higher frequency, dynamic character of these materials was highlighted by the cross-over between storage and loss modulus in both reinforced and unreinforced materials. All materials showed good stress relaxation properties, even under ambient conditions due to hydrogen bonded UPy units[51,52] as well as TM linkages.[55,56] Figure 3b shows that poly(EA_{150}-$UPyMA_{3.75}$-$FMA_{3.75}$-$Thiol_{3.75}$) materials relaxed over 90% of the initial stress within 150 min under ambient conditions, and over 80% of peak stress relaxed in the material reinforced with 0.9 wt% MWCNT. Although both reinforced and matrix only materials showed excellent stress relaxation, the higher modulus and stiffness resulting from reinforcement rigidified materials decreased the stress relaxation rate and plateau value in all reinforced materials (Figure S8). Stress relaxation observed in these materials can be attributed to the presence of multiple types of macromolecular engineered dynamic bonds. To confirm the influence of hydrogen bonding on the stress relaxation observed, MWCNT-reinforced and unreinforced dual-dynamic poly(EA_{150}-$Thiol_{5.6}$-$FMA_{5.6}$) was synthesized and studied as control materials that lack contribution from hydrogen bonding. Control systems were cross-linked with BMI through dynamic DA and TM chemistries based on the design principle for triply-dynamic systems. Figure S9 reveals that only ~60% of the stress applied to poly(EA_{150}-$Thiol_{5.6}$-$FMA_{5.6}$) was relaxed compared to ~ 90% stress relaxation observed in poly(EA_{150}-$UPyMA_{3.75}$-$Thiol_{3.75}$-$FMA_{3.75}$). This suggests that dynamic hydrogen bonds contribute significantly to the stress relaxation observed in triply-dynamic materials.

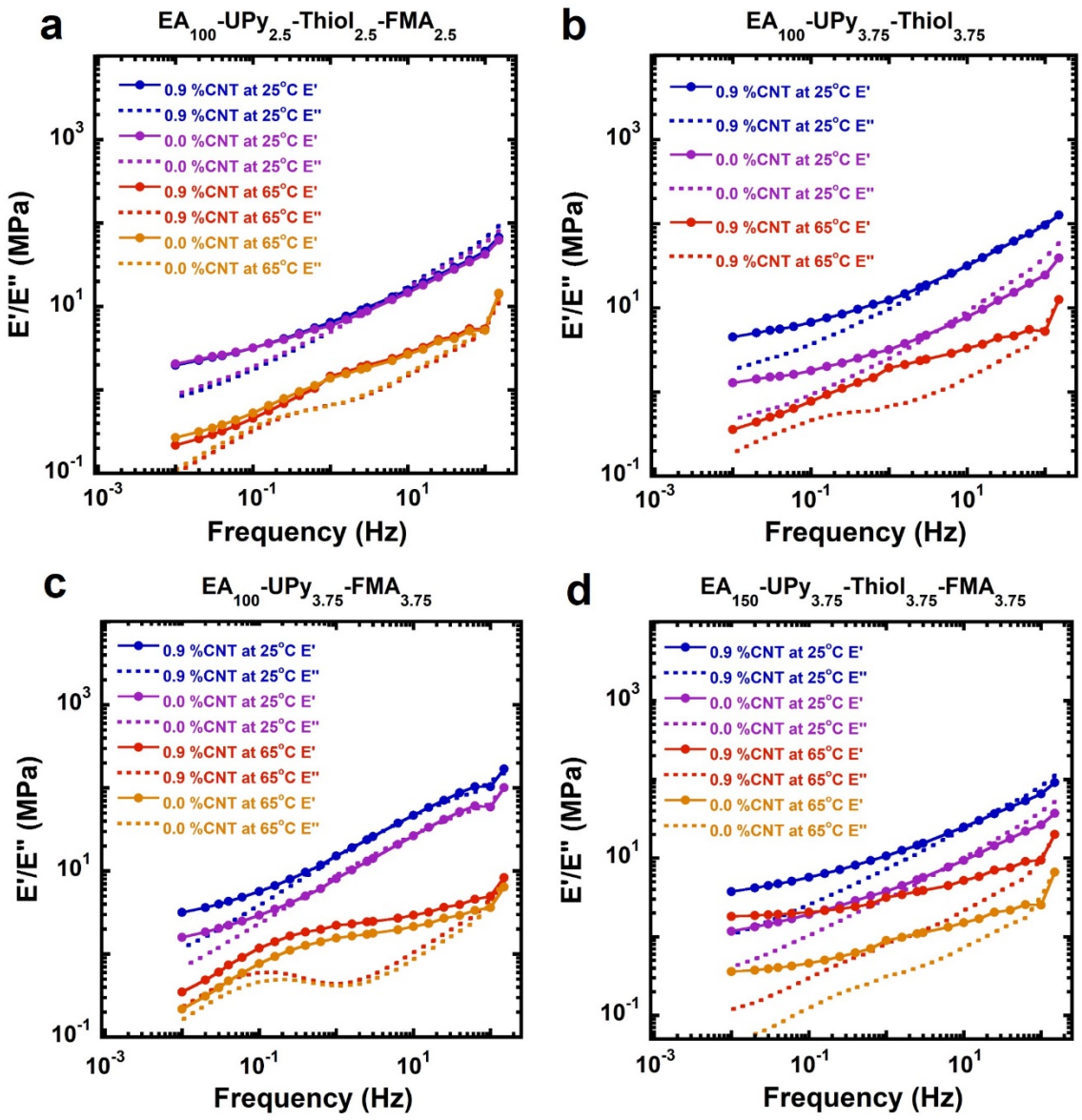

Figure 4. Combined frequency sweeps of reinforced and unreinforced (a) dual-dynamic poly(EA_{100}-$UPyMA_{3.75}$-$FMA_{3.75}$), (b) dual-dynamic poly(EA_{100}-$UpyMA_{3.75}$-$Thiol_{3.75}$), (c) triply-dynamic poly(EA_{100}-$UpyMA_{2.5}$-$FMA_{2.5}$-$Thiol_{2.5}$), and (d) triply-dynamic poly(EA_{150}-$UpyMA_{3.75}$-$FMA_{3.75}$-$Thiol_{3.75}$) at 25 and 65 °C.

Figure 4 presents frequency sweeps for reinforced and unreinforced dual-dynamic poly(EA_{100}-$UPyMA_{3.75}$-$FMA_{3.75}$), dual-dynamic poly(EA_{100}-$UPyMA_{3.75}$-$Thiol_{3.75}$), triply-dynamic poly(EA_{100}-$UPyMA_{2.5}$-$FMA_{2.5}$-$Thiol_{2.5}$), and triply-dynamic poly(EA_{150}-$UPyMA_{3.75}$-$FMA_{3.75}$-$Thiol_{3.75}$) all carried out at 25 and 65 °C using 0.3% applied strain respectively. In all four

systems, it was observed that higher temperature led to lower storage moduli, hence highlighting thermoresponsive behavior in all materials. This is consistent with dynamic polymer materials based on covalent TM,[56] furan-maleimide DA,[58] and dynamic hydrogen bonds[23] reported in literature, and is likely due to dissociation and faster exchange from hydrogen bonded UPy units. Figure S10 gives a holistic view of combined frequency sweep data for experiments conducted at 25, 45, and 65 °C, showing a general progressive decrease in moduli as experimental temperature increases respectively. Dual-dynamic poly(EA_{100}-$UPyMA_{3.75}$-$FMA_{3.75}$) gave a slightly higher storage moduli compared to poly(EA_{100}-$UPyMA_{3.75}$-$Thiol_{3.75}$) especially at higher frequency (Figure 4a-b, S11a). Triply-dynamic with longer chain lengths, poly(EA_{150}-$UPyMA_{3.75}$-$FMA_{3.75}$-$Thiol_{3.75}$) represented in Figure 4d and poly(EA_{200}-$UPyMA_{5.00}$-$Thiol_{5.00}$-$FMA_{5.00}$) represented in Figure S11b had larger increase in storage modulus upon introduction of 0.9% MWCNTs compared to the shorter-chain poly(EA_{100}-$UPyMA_{2.5}$-$FMA_{2.5}$-$Thiol_{2.5}$) shown in Figure 4c. This could be due to longer chain lengths facilitating more elastically effective connections between the MWCNT and the matrix, with potentially fewer intramolecular loops formed.

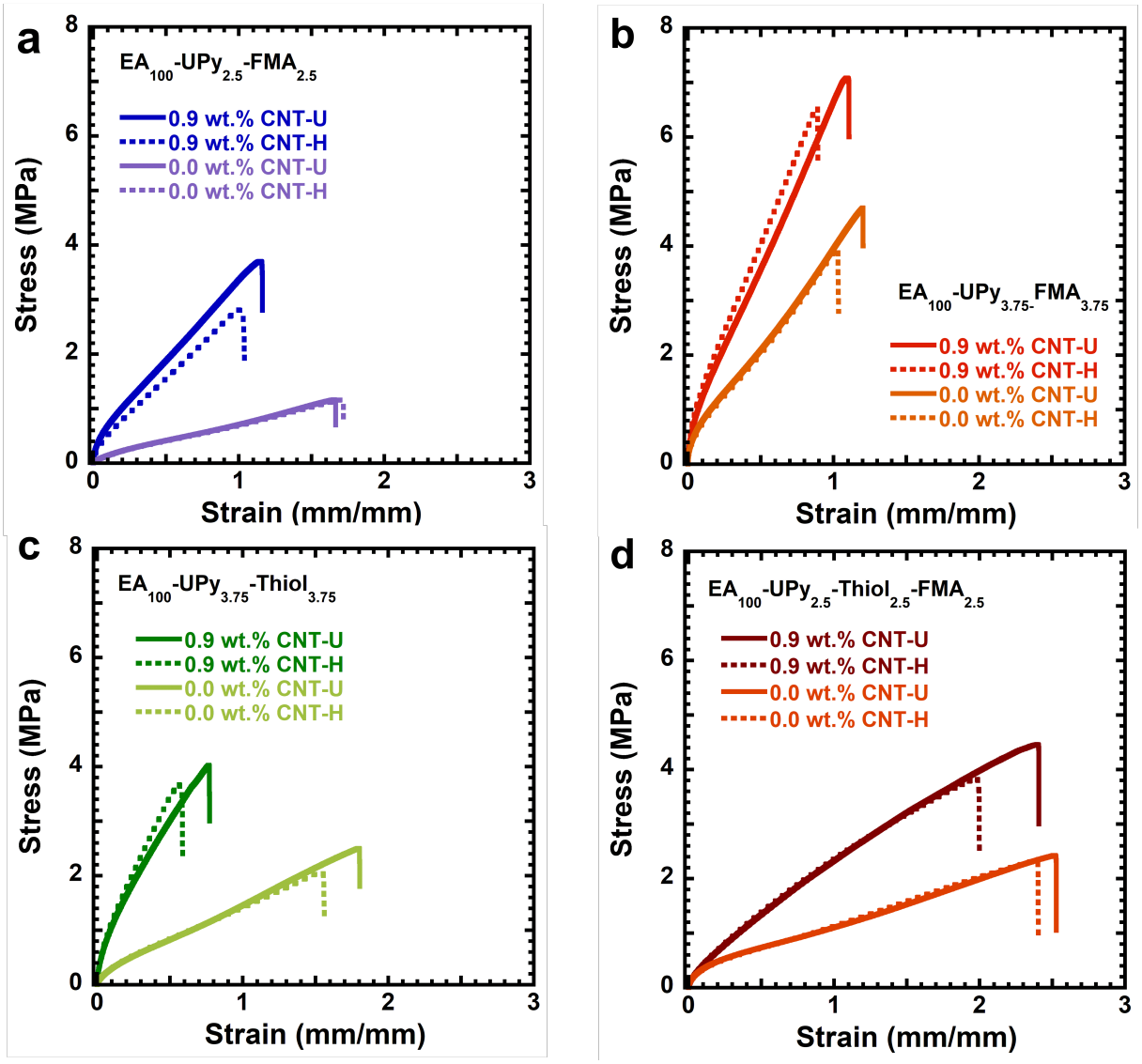

Figure 5. Stress-strain curves for reinforced and unreinforced (a) dual-dynamic poly(EA_{100}-$UPyMA_{2.5}$-$FMA_{2.5}$), (b) dual-dynamic poly(EA_{100}-$UPyMA_{3.75}$-$FMA_{3.75}$), (c) dual-dynamic poly(EA_{100}-$UPyMA_{3.75}$-$Thiol_{3.75}$), and (d) triply-dynamic poly(EA_{100}-$UPyMA_{2.50}$-$Thiol_{2.50}$-$FMA_{2.50}$). Uncut pristine polymer samples are represented with a 'U' and healed samples are represented with 'H'.

Tensile tests were used to evaluate material properties and determine self-healing and dynamic exchange potential of each material. Young's modulus (Y) was obtained using the Ogden model.[59] Toughness (Φ) was evaluated by integrating the engineering stress from a strain of 0 until break. Average values for peak stress (σ_{peak}), strain at break (ε_{break}), and Y of all materials are shown in Table 1. Tensile testing curves are reported in Figure 5. It was observed that addition of

less than 1 wt.% MWCNT gave substantial increase in materials strength across all systems. Doubly dynamic 7.5% cross-linked Poly(EA_{100}-$UPyMA_{3.75}$-$FMA_{3.75}$) showed improved strength (with over 100% increase in stress) and toughness compared to less cross-linked poly(EA_{100}-$UPyMA_{2.5}$-$FMA_{2.5}$) which reached higher strain (Figure 5a-b). This may be due to the presence of more cross-linking sites in poly(EA_{100}-$UPyMA_{3.75}$-$FMA_{3.75}$) resulting in a stronger material. Thermal healing and reinforcement in both materials are comparable, where material healability is observed due to the presence of dynamic hydrogen bonds, thermo-responsive DA, and TM adducts as dynamic linkages. Doubly dynamic 7.5% cross-linked Poly(EA_{100}-$UPyMA_{3.75}$-$Thiol_{3.75}$) showed better healing (Figure 5c), extensibility, and generally ~40% less strength compared to poly(EA_{100}-$UPyMA_{3.75}$-$FMA_{3.75}$) (Figure 5b). Although interestingly, addition of MWCNT led to improved strength (~55% increased stress) and toughness (~40% less strain) in poly(EA_{100}-$UPyMA_{3.75}$-$Thiol_{3.75}$). This was probably due to steric effect between polymer matrix and MWCNTs. Another possibility is that during self-healing, materials cured at 90 °C could lead to fast exchanges between TM linkages within the system. Although equilibrium in this process favors formation of TM linkages (Figure 2), it is possible that one end of BMI cross-linker could undergo Thiol-Michael addition with a thiol group on the polymer and the other end undergoes DA chemistry with MWCNT, ultimately resulting in effective reinforcement.[40] Unlike dual-dynamic materials, 7.5% cross-linked triply-dynamic poly(EA_{100}-$UPyMA_{2.5}$-$Thiol_{2.5}$-$FMA_{2.5}$) showed that reinforcement can be achieved without necessarily losing extensibility (Figure 5d). Reinforced poly(EA_{100}-$UPyMA_{2.5}$-$Thiol_{2.5}$-$FMA_{2.5}$) had an average ε_{break} of ~2.20 mm/mm which is greater than all average ε_{break} observed in Figure 5a-c (Table 1). Also, MWCNT enhanced poly(EA_{100}-$UPyMA_{2.5}$-$Thiol_{2.5}$-$FMA_{2.5}$) showed substantial reinforcement with ~80% increase in stress compared to their unreinforced materials. This could be due to DA adducts of furan diene and π-bonds on MWCNT surface, TM adduct of thiol and BMI, and hydrogen-bonds from UPy motifs. Unique roles of different groups present in the triple network allows resulting materials to possess properties observed in both dual-dynamic poly(EA_{100}-$UPyMA_{3.75}$-$FMA_{3.75}$) and poly(EA_{100}-$UPyMA_{3.75}$-$Thiol_{3.75}$).

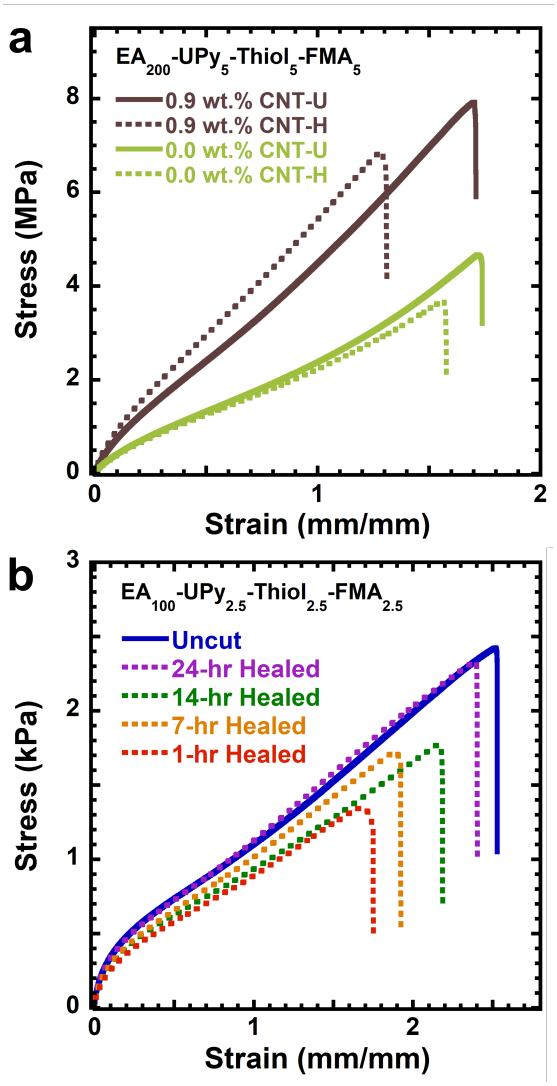

Figure 6: (a) Stress-strain curves for reinforced and unreinforced poly(EA_{200}-$UPyMA_5$-$Thiol_5$-FMA_5). (b) Varied self-healing time stress-strain curves for unreinforced poly(EA_{100}-$UPyMA_{2.5}$-$Thio_{2.5}$-$FMA_{2.5}$).

Overall, healability and extensibility is observed in triply-dynamic networks with reinforced variants showing increased strength while retaining extensibility that is comparable to unreinforced variants as shown in Figure 5d and Figure 6a. Additionally, longer chain triply-dynamic DP200 reinforced poly(EA_{200}-$UPyMA_5$-$Thiol_5$-FMA_5) materials gave average σ_{peak} of ~8 MPa compared to ~6 MPa and ~4 MPa in DP150 poly(EA_{150}-$UPyMA_{3.75}$-$Thiol_{3.75}$-$FMA_{3.75}$) and DP100 poly(EA_{100}-$UPyMA_{2.5}$-$Thiol_{2.5}$-$FMA_{2.5}$) respectively (Figure S12, Table 1). Time evolution of the self-healing efficiency of poly(EA_{100}-$UPyMA_{2.5}$-$Thio_{2.5}$-$FMA_{2.5}$) showed

approximately 60% recovery of mechanical properties within 1 hour of heating at 90 °C. The is likely because approximately half the dynamic linkages are fast exchanging hydrogen bonded UPy units, hence longer healing times led to overall better healing as illustrated in Figure 6b. This is an impressively fast time scale of healing considering it takes another 23 hours to achieve only ~35% more recovery. This is an improvement compared to our previous report[40] where approximately 80% thermal healing was achieved after treatment for 24 hours at 90 °C and no significant healing was observed after 1 hour due to absence of complementary orthogonal dynamic bonds.

Thermosets are highly cross-linked covalent networks, which makes reprocessing a major challenge.[60] Thermosets have a wide range of applications ranging from auto-parts and aerospace materials to insulation handles for kitchen wares.[60,61] Upon failure however, thermosets cannot be repaired or recycled and that consequently reduces their service life, leading to a waste of resources. Thus, designing malleable and thermally repairable polymer nanocomposites which can undergo multiple recycling without losing network integrity is important for materials applications. DA reaction has been well studied as a covalent adaptable network mainly targeted towards achieving repairable polymers[62] and even in fabrication of fiber-reinforced polymer materials.[63] This implies that introducing dynamic bonds into polymers or polymer composites can lead to thermosets with reprocessable properties. Figure 7a demonstrates the reprocessability of DPNs in this study by hot pressing. Typical reinforced material (with 0.9 wt.% CNT) and unreinforced material (without CNT) were shown to successfully undergo remolding multiple times at 100 °C for 1 hr, similar to remolding conditions used by Guo *et. al* to reprocess a CNT–vitrimer composite.[64] Recyclability of these DPNs is due to simultaneous dynamic hydrogen bonds, DA reversibility, and partially by TM exchange reaction activated at elevated temperature. No significant loss in tensile property of materials was observed after reprocessing three times (Figure 6b-e). The data in Figure 7 indicate that these materials could pave the way for designing less expensive but yet highly effective next generation self-healing carbon/polymer composites for aerospace and automotive materials,[61] especially since less than 1 wt.% of nanocomposite material is required.

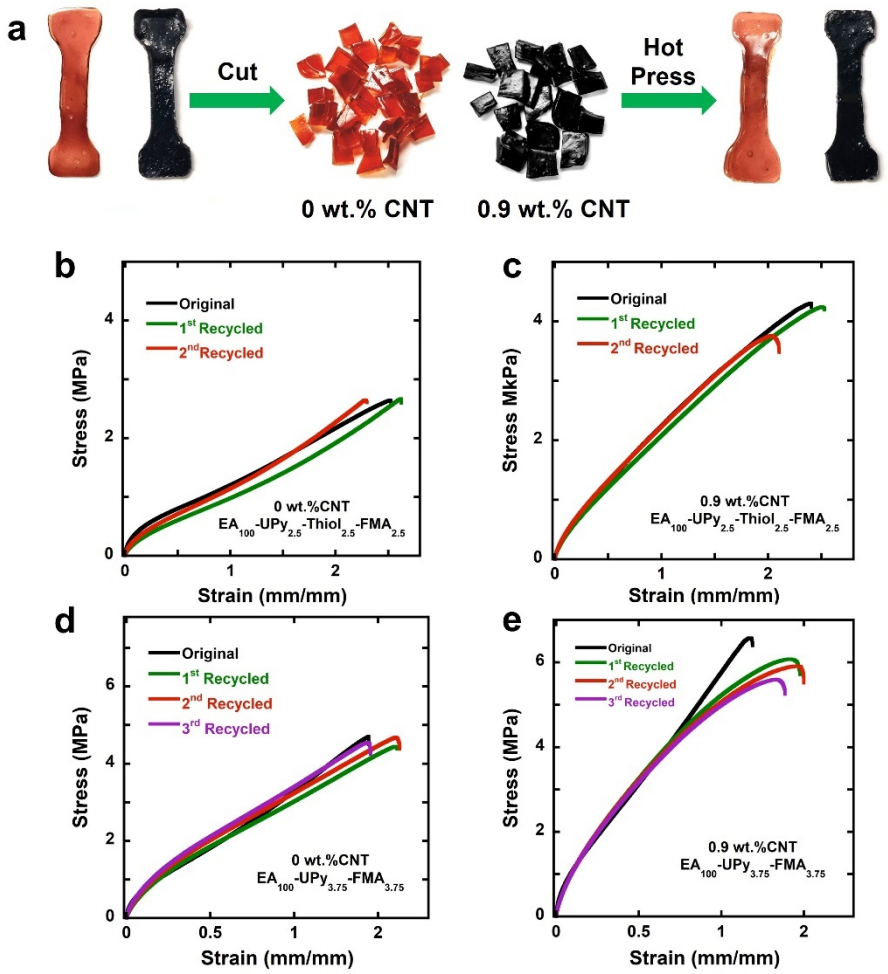

Figure 7. (a) Photographs showing the reprocessing steps for a typical unreinforced (0 wt.% CNT) and reinforced (0.9 wt.% CNT) DPN. (b) Strain-strain curves of original and recycled CNT reinforced EA_{100}-$UPy_{2.5}$-$Thiol_{2.5}$-$FMA_{2.5}$ (c) unreinforced EA_{100}-$UPy_{2.5}$-$Thiol_{2.5}$-$FMA_{2.5}$ (d) CNT reinforced EA_{100}-$UPy_{3.75}$-$FMA_{3.75}$ (e) unreinforced EA_{100}-$UPy_{3.75}$-$FMA_{3.75}$.

Scanning electron microscopy was used to explore the morphology of typical reinforced and unreinforced triply-dynamic materials (Figure 8a-d). An interesting phenomenon showed that unreinforced materials reveal smooth surfaces even when fractured (Figures 8a-b, S13). This is contrary to reinforced materials which show evidence of MWCNT tiny colonies that can be observed on the surface (Figure 8c) and MWCNT distribution when fractured (Figure 8d). The presence of MWCNT in poly(EA_{100}-$UPyMA_{2.5}$-$Thio_{2.5}$-$FMA_{2.5}$) shows the visual effect of nano-reinforcement on the material morphology and give some insight into the distribution of

nanocomposites in the polymer matrix. Electrical conductivity (κ) of all reinforced materials was obtained using a four-point probe (Figure 9) as illustrated in Figure S4. Unreinforced materials were not tested because they cannot reach electrical percolation, hence do not provide measurable electrical current.[40] Generally, since electrical percolation is less impacted by chain bridging in polymer architecture, all DPNs in this study showed electrical conductivities in the order of 10^{-5}–10^{-4} S/m due to only less than 1 wt.% MWCNT nanoreinforcement (Figure 7f). Suggesting that these DPNs could potentially contribute to the rapidly growing fields of flexible compliant electrodes[65] and strain sensors.[45]

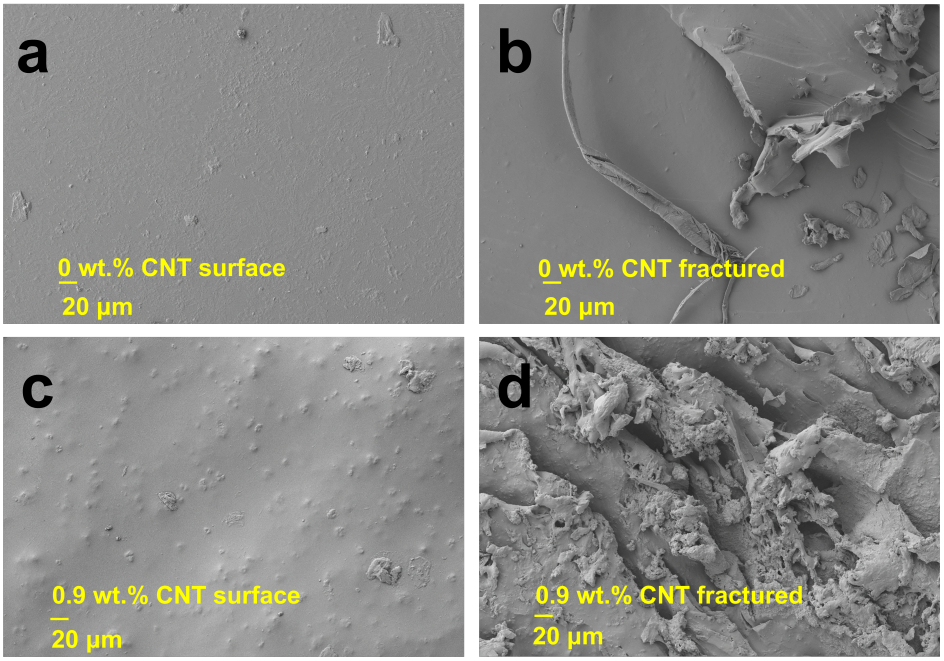

Figure 8. Scanning electron micrographs of triply-dynamic poly(EA_{100}-$UPyMA_{2.5}$-$Thio_{2.5}$-$FMA_{2.5}$) with 20 µm scale bars and 200X magnification showing (a) surface and (b) razor-sliced interior of unreinforced materials then (c) surface and (d) razor-sliced interior of reinforced materials.

In the future, scientists envisage that human senses will be greatly enhanced by electronics that are built into accessories, clothes, and sensors attached to the skin. This has influenced the high demand in wearable electronics such as flexible compliant electrodes[66] and strain sensors.[45] For example, common uses of strain sensors include artificial skins, health monitoring devices,

strain gauges, etc.[67] To truly benefit from wearable operations, it is highly desired that stretchability and flexibility are well engineered into wearable systems. Hence our contribution in this work provides a potential pathway to retaining stretchability and flexibility in polymer-composite electronic sensors. Additionally, cracks and damage in large structures (e.g., airplanes, submarines, wind turbines, etc.) can be detected using flexible electronics that are capable of measuring large strain. For example, large-area flexible sensing materials could be used in very practical applications like sensing premature cracking on an aircraft body which could enable the replacement of damaged parts during routine service, hence preventing the occurrence of life-threatening situations during flight.[68] Challenges associated to such flexible polymer-composite electrodes and strain sensors include micro-cracks (or premature fracture) within polymer layer and reduced material durability due to ageing. These damages are highly minimized in materials with self-healing ability.[69]

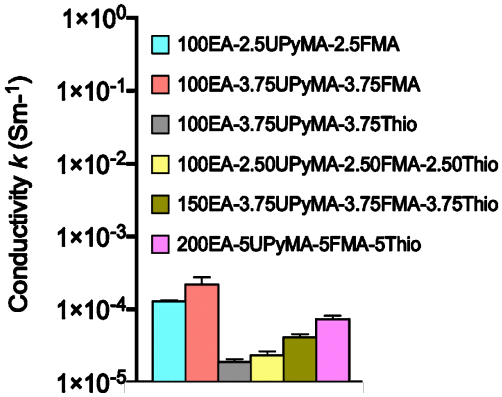

Figure 9. Electrical conductivity (κ) profile of all materials reinforced with 0.9 wt.% MWCNT.

Summary and Conclusions

In this study, we proposed a solution to a common problem associated to polymer composite materials. Where direct reinforcement of polymer materials using nanocomposites leads to enhanced mechanical properties in resulting polymer composites but poor dynamic character such as self-healing and reprocessability, suggesting a trade-off between enhanced mechanical properties and dynamic character in such materials.[44] To address this problem, we proposed that single network polymers with up to three types of orthogonal dynamic bonds could potentially

provide solution to the trade-off problem due to the presence of complimentary dynamic interactions. We demonstrated that addition of <1 wt.% of MWCNT led to covalent bonding between the polymer network and composite via DA adduct and ultimately effective reinforcement of the resulting DPN without significant loss in dynamic character. Owing to the addition of MWCNT, triple-dynamic materials showed dynamic properties such as healability and reprocessability despite increased material strength. Reinforced and unreinforced materials show no significant difference in the number of times each material can be recycled. Also, we demonstrated using stress-strain data in Figure 5 and toughness data in Table 1 that there is no difference in the elongation of reinforced materials compared to the unreinforced ones despite the reinforced materials having increased toughness. This indicates material resilience and their future promise as excellent candidates for high performing mechanically robust materials. Combining unique dynamic covalent chemistries resulted in triply-dynamic polymer composites with over 3 MPa increase in stress and 4 MPa increase in Young's modulus compared to unreinforced materials. In addition to electrical conductivity, dynamic properties such as healability, stress relaxation, thermoresponsive behavior, and recyclability were achieved across all materials, hence paving the way for designing next-generation of sustainable polymer composites that could be useful for aerospace and automotive parts, as well as medical devices.

ASSOCIATED CONTENT

Supporting Information

Experimental materials and procedures, small molecule study monitored using ^{1}H NMR, material characterization and analytical methods, and additional supplemental data.

AUTHOR INFORMATION

Corresponding Author

Dominik Konkolewicz – *Department of Chemistry and Biochemistry, Miami University, 651 E. High Street, Oxford, Ohio 45056, United States;* Email: d.konkolewicz@MiamiOH.edu

Authors

Obed J. Dodo – *Department of Chemistry and Biochemistry, Miami University, 651 E. High Street, Oxford, Ohio 45056, United States*

Leilah Petit – *Department of Chemistry and Biochemistry, Miami University, 651 E. High Street, Oxford, Ohio 45056, United States*

Derrick Dunn – *Department of Chemistry and Biochemistry, Miami University, 651 E. High Street, Oxford, Ohio 45056, United States*

Camaryn P. Myers – *Department of Chemistry and Biochemistry, Miami University, 651 E. High Street, Oxford, Ohio 45056, United States*

Notes

The authors declare no competing interest.

Funding

We are grateful to the National Science Foundation (NSF) for partially supporting this work under Grant No. DMR-1749730 (Supporting O.J.D for conceptualization, material synthesis, characterization, and manuscript development; C.M and D.D for material synthesis; and D.K. for conceptualization and manuscript development). Partial support from NSF Grant No. CHE-1851795 supporting L.P. (REU in Chemistry at Miami University) for material synthesis is also duly acknowledged. 400 MHz NMR instrumentation at Miami University is supported through funding from the NSF under grant number (CHE-1919850). Findings, conclusions, and recommendations described in this material do not necessarily reflect the views of the NSF but instead those of the authors. Dominik Konkolewicz would also like to acknowledge the support from the Robert H. and Nancy J. Blayney Professorship.

ACKNOWLEDGEMENTS

We are thankful to Nethmi De Alwis and Ibrahim Oladayo Raji for experimental assistance.

ABBREVIATIONS

DA, Diels-Alder; TM, thiol-Michael; UPy, 2-ureido-4[1H]-pyrimidinone; DPNs, dynamic polymer nanocomposites; CNTs, carbon nanotubes; MWCNTs, multiwalled carbon nanotubes; UPyMA, 2-ureido-4[1H]-pyrimidinone-methyl-acrylate; FMA, furfuryl methacrylate; EXEA, ethyl xanthate ethyl acrylate; EA, ethyl acrylate; BMI, 1,1′-(methylenedi-4,1-phenylene)-bismaleimide; FA, furfuryl alcohol; DMA, dynamic mechanical analyzer; DSC, differential scanning calorimetry; and TGA, thermogravimetric analysis.

REFERENCES

(1) Gomez, E. F.; Wanasinghe, S. V.; Flynn, A. E.; Dodo, O. J.; Sparks, J. L.; Baldwin, L. A.; Tabor, C. E.; Durstock, M. F.; Konkolewicz, D.; Thrasher, C. J. 3D-Printed Self-Healing Elastomers for Modular Soft Robotics. *ACS Appl. Mater. Interfaces* **2021**, *13* (24), 28870–28877. https://doi.org/10.1021/acsami.1c06419.

(2) Song, Y.; Liu, Y.; Qi, T.; Li, G. L. Towards Dynamic but Super Tough Healable Polymers through Bio-Mimetic Hierarchical Hydrogen - Bonding Interactions. *Angew. Chemie Int. Ed.* **2018**, *57* (42), 13838–13842. https://doi.org/10.1002/anie.201807622.

(3) Xu, J.; Chen, P.; Wu, J.; Hu, P.; Fu, Y.; Jiang, W.; Fu, J. Notch-Insensitive, Ultrastretchable, Efficient Self-Healing Supramolecular Polymers Constructed from Multiphase Active Hydrogen Bonds for Electronic Applications. *Chem. Mater.* **2019**, *31* (19), 7951–7961. https://doi.org/10.1021/acs.chemmater.9b02136.

(4) Tee, B. C. K.; Wang, C.; Allen, R.; Bao, Z. An Electrically and Mechanically Self-Healing Composite with Pressure- and Flexion-Sensitive Properties for Electronic Skin Applications. *Nat. Nanotechnol.* **2012**, *7* (12), 825–832. https://doi.org/10.1038/nnano.2012.192.

(5) Ulijn, R. V.; Bibi, N.; Jayawarna, V.; Thornton, P. D.; Todd, S. J.; Mart, R. J. .; Smith, A. M.; Gough, J. E. Bioresponsive Hydrogels. *Mater. Today* **2007**, *10* (4), 40–48. https://doi.org/10.1016/S1369-7021(07)70049-4.

(6) Podual, K.; Doyle III, F. J.; Peppas, N. A. Preparation and Dynamic Response of Cationic

Copolymer Hydrogels Containing Glucose Oxidase. *Polymer (Guildf).* **2000**, *41* (11), 3975–3983. https://doi.org/10.1016/S0032-3861(99)00620-5.

(7) Kuang, X.; Mu, Q.; Roach, D. J.; Jerry Qi, H. Shape-Programmable and Healable Materials and Devices Using Thermo- And Photo-Responsive Vitrimer. *Multifunct. Mater.* **2020**, *3* (4). https://doi.org/10.1088/2399-7532/abbdc1.

(8) Duan, L.; Lai, J. C.; Li, C. H.; Zuo, J. L. A Dielectric Elastomer Actuator That Can Self-Heal Integrally. *ACS Appl. Mater. Interfaces* **2020**, *12* (39), 44137–44146. https://doi.org/10.1021/acsami.0c11697.

(9) Liu, W.; Zhang, B.; Lu, W. W.; Li, X.; Zhu, D.; Yao, K. De; Wang, Q.; Zhao, C.; Wang, C. A Rapid Temperature-Responsive Sol-Gel Reversible Poly(N- Isopropylacrylamide)-g-Methylcellulose Copolymer Hydrogel. *Biomaterials* **2004**, *25* (15), 3005–3012. https://doi.org/10.1016/j.biomaterials.2003.09.077.

(10) De Alwis, W. N.; Ahammed, B.; Dolan, M. T. .; Fang, Q.; Wu, J.; Sparks, J. L.; Zanjani, M. B.; Konkolewicz, D. .; Ye, Z. Accelerating Dynamic Exchange and Self-Healing Using Mechanical Forces in Crosslinked Polymers. *Mater. Horizons* **2020**, *7* (6), 1581–1587. https://doi.org/10.1039/c9mh01938c.

(11) Zhang, W.; Jin, Y. Dynamic Covalent Chemistry : Principles, Reactions, and Applications. *Wiley Online Libr.* **2017**, 464–461. https://doi.org/10.1002/9781119075738.

(12) Otsuka, H.; Aotani, K.; Higaki, Y.; Takahara, A. Polymer Scrambling: Macromolecular Radical Crossover Reaction between the Main Chains of Alkoxyamine-Based Dynamic Covalent Polymers. *J. Am. Chem. Soc.* **2003**, *125* (14), 4064–4065. https://doi.org/10.1021/ja0340477.

(13) Cash, J. J.; Kubo, T.; Bapat, A. P.; Sumerlin, B. S. Room-Temperature Self-Healing Polymers Based on Dynamic-Covalent Boronic Esters. *Macromolecules* **2015**, *48* (7), 2098–2106. https://doi.org/10.1021/acs.macromol.5b00210.

(14) Lei, Z. Q.; Xiang, H. P.; Yuan, Y. J.; Rong, M. Z.; Zhang, M. Q. Room-Temperature Self-Healable and Remoldable Cross-Linked Polymer Based on the Dynamic Exchange of Disulfide Bonds. *Chem. Mater.* **2014**, *26* (6), 2038–2046.

https://doi.org/10.1021/cm4040616.

(15) Mukherjee, S.; Bapat, A. P.; Hill, M. R.; Sumerlin, B. S. Oximes as Reversible Links in Polymer Chemistry: Dynamic Macromolecular Stars. *Polym. Chem.* **2014**, *5* (24), 6923–6931. https://doi.org/10.1039/c4py01282h.

(16) Reutenauer, P.; Buhler, E.; Boul, P. J.; Candau, S. J.; Lehn, J. M. Room Temperature Dynamic Polymers Based on Diels-Alder Chemistry. *Chem. - A Eur. J.* **2009**, *15* (8), 1893–1900. https://doi.org/10.1002/chem.200802145.

(17) Kim, K. S.; Cho, H. J.; Lee, J.; Ha, S.; Song, S. G.; Kim, S.; Yun, W. S.; Kim, S. K.; Huh, J.; Song, C. Dynamic Covalent Hydrazone Supramolecular Polymers toward Multiresponsive Self-Assembled Nanowire System. *Macromolecules* **2018**, *51* (20), 8278–8285. https://doi.org/10.1021/acs.macromol.8b01909.

(18) Kathan, M.; Jurissek, C.; Kovaříček, P.; Hecht, S. Imine-Based Dynamic Polymer Networks as Photoprogrammable Amine Sensing Devices. *J. Polym. Sci. Part A Polym. Chem.* **2019**, *57* (24), 2378–2382. https://doi.org/10.1002/pola.29518.

(19) Li, Y.; Rios, O.; Keum, J. K.; Chen, J.; Kessler, M. R. Photoresponsive Liquid Crystalline Epoxy Networks with Shape Memory Behavior and Dynamic Ester Bonds. *ACS Appl. Mater. Interfaces* **2016**, *8* (24), 15750–15757. https://doi.org/10.1021/acsami.6b04374.

(20) Hatai, J.; Hirschhäuser, C.; Niemeyer, J.; Schmuck, C. Multi-Stimuli-Responsive Supramolecular Polymers Based on Noncovalent and Dynamic Covalent Bonds. *ACS Appl. Mater. Interfaces* **2020**, *12* (2), 2107–2115. https://doi.org/10.1021/acsami.9b19279.

(21) Lue, Xiang; Liu, Xianfeng; Zhang, Huan; Zhaoab, Ning; Zhang, K. Thermoresponsive Self-Healable and Recyclable Polymer Networks Based on a Dynamic Quinone Methide-Thiol Chemistry. *Polym. Chem.* **2020**, *11*, 6157–6162. https://doi.org/10.1039/D0PY01008A.

(22) Rybtchinski, B. Adaptive Supramolecular Nanomaterials Based on Strong Noncovalent Interactions. *ACS Nano* **2011**, *5* (9), 6791–6818. https://doi.org/10.1021/nn2025397.

(23) Cummings, S. C.; Dodo, O. J.; Hull, A. C.; Zhang, B.; Myers, C. P.; Sparks, J. L.; Konkolewicz, D. Quantity or Quality: Are Self-Healing Polymers and Elastomers Always

Tougher with More Hydrogen Bonds? *ACS Appl. Polym. Mater.* **2020**, *2* (3), 1108–1113. https://doi.org/10.1021/acsapm.9b01095.

(24) Ramakrishna, S.; Mayer, J.; Wintermantel, E.; Leong, K. W. Biomedical Applications of Polymer-Composite Materials: A Review. *Compos. Sci. Technol.* **2001**, *61* (9), 1189–1224. https://doi.org/10.1016/S0266-3538(00)00241-4.

(25) Chow, W. S.; Mohd Ishak, Z. A. Smart Polymer Nanocomposites: A Review. *Express Polym. Lett.* **2020**, *14* (5), 416–435. https://doi.org/10.3144/expresspolymlett.2020.35.

(26) Ciecierska, E.; Boczkowska, A.; Kurzydlowski, K. J.; Rosca, I. D.; Van Hoa, S. The Effect of Carbon Nanotubes on Epoxy Matrix Nanocomposites. *J. Therm. Anal. Calorim.* **2013**, *111* (2), 1019–1024. https://doi.org/10.1007/s10973-012-2506-0.

(27) Tarfaoui, M.; Lafdi, K.; El Moumen, A. Mechanical Properties of Carbon Nanotubes Based Polymer Composites. *Compos. Part B Eng.* **2016**, *103*, 113–121. https://doi.org/10.1016/j.compositesb.2016.08.016.

(28) Thakur, V. K.; Kessler, M. R. Self-Healing Polymer Nanocomposite Materials: A Review. *Polymer (Guildf).* **2015**, *69*, 369–383. https://doi.org/10.1016/j.polymer.2015.04.086.

(29) Olugebefola, S. C.; Hamilton, A. R.; Fairfield, D. J.; Sottos, N. R.; White, S. R. Structural Reinforcement of Microvascular Networks Using Electrostatic Layer-by-Layer Assembly with Halloysite Nanotubes. *Soft Matter* **2013**, *10*, 544–548. https://doi.org/10.1039/C3SM52288A.

(30) White, S. R.; Sottos, N. R.; Geubelle, P. H.; Moore, J. S.; Kessler, M. R.; Sriram, S. R.; Brown, E. N.; Viswanathan, S. Autonomic Healing of Polymer Composites. *Nature* **2001**, *409*, 794–797. https://doi.org/10.1038/35057232.

(31) Herbst, F.; Döhler, D.; Michael, P.; Binder, W. H. Self-Healing Polymers via Supramolecular Forces. *Macromol. Rapid Commun.* **2013**, *34* (3), 203–220. https://doi.org/10.1002/marc.201200675.

(32) Chakma, P.; Konkolewicz, D. Dynamic Covalent Bonds in Polymeric Materials. *Angew. Chemie - Int. Ed.* **2019**, *131* (29), 9784–9797. https://doi.org/10.1002/ange.201813525.

(33) Engel, T.; Kickelbick, G. Self-Healing Nanocomposites from Silica-Polymer Core-Shell Nanoparticles. *Polym. Int.* **2014**, *63* (5), 915–923. https://doi.org/10.1002/pi.4642.

(34) Xiao, X.; Xie, T.; Cheng, Y. T. Self-Healable Graphene Polymer Composites. *J. Mater. Chem.* **2010**, *20* (17), 3508–3514. https://doi.org/10.1039/c0jm00307g.

(35) Idumah, C. I.; Odera, S. R. Recent Advancement in Self-Healing Graphene Polymer Nanocomposites, Shape Memory, and Coating Materials. *Polym. Technol. Mater.* **2020**, *59* (11), 1167–1190. https://doi.org/10.1080/25740881.2020.1725816.

(36) Bellucci, S.; Coderoni, L.; Micciulla, F.; Rinaldi, G.; Sacco, I. The Electrical Properties of Epoxy Resin Composites Filled with Cnts and Carbon Black. *J. Nanosci. Nanotechnol.* **2011**, *11* (10), 9110–9117. https://doi.org/10.1166/jnn.2011.4281.

(37) Chang, C. M.; Liu, Y. L. Functionalization of Multi-Walled Carbon Nanotubes with Furan and Maleimide Compounds through Diels-Alder Cycloaddition. *Carbon N. Y.* **2009**, *47* (13), 3041–3049. https://doi.org/10.1016/j.carbon.2009.06.058.

(38) Zydziak, N.; Preuss, C. M.; Winkler, V.; Bruns, M.; Hübner, C.; Barner-Kowollik, C. Hetero Diels-Alder Chemistry for the Functionalization of Single-Walled Carbon Nanotubes with Cyclopentadienyl End-Capped Polymer Strands. *Macromol. Rapid Commun.* **2013**, *34* (8), 672–680. https://doi.org/10.1002/marc.201300025.

(39) Zydziak, N.; Hübner, C.; Bruns, M.; Barner-Kowollik, C. One-Step Functionalization of Single-Walled Carbon Nanotubes (SWCNTs) with Cyclopentadienyl-Capped Macromolecules via Diels-Alder Chemistry. *Macromolecules* **2011**, *44* (9), 3374–3380. https://doi.org/10.1021/ma200107z.

(40) Stopler, E. B.; Dodo, O. J.; Hull, A. C.; Weaver, K. A.; Chakma, P.; Edelmann, R.; Ranly, L.; Zanjani, M. B.; Ye, Z.; Konkolewicz, D. Carbon Nanotube Enhanced Dynamic Polymeric Materials through Macromolecular Engineering. *Mater. Adv.* **2020**, *1* (5), 1071–1076. https://doi.org/10.1039/d0ma00143k.

(41) Zhang, B.; Ke, J.; Vakil, J. R.; Cummings, S. C.; Digby, Z. A.; Sparks, J. L.; Ye, Z.; Zanjani, M. B.; Konkolewicz, D. Dual-Dynamic Interpenetrated Networks Tuned through Macromolecular Architecture. *Polym. Chem.* **2019**, *10* (46), 6290–6304.

https://doi.org/10.1039/c9py01387c.

(42) Hammer, L.; Van Zee, N. J.; Nicolaÿ, R. Dually Crosslinked Polymer Networks Incorporating Dynamic Covalent Bonds. *Polymers (Basel).* **2021**, *13* (3), 1–34. https://doi.org/10.3390/polym13030396.

(43) Foster, E. M.; Lensmeyer, E. E.; Zhang, B.; Chakma, P.; Flum, J. A.; Via, J. J.; Sparks, J. L.; Konkolewicz, D. Effect of Polymer Network Architecture, Enhancing Soft Materials Using Orthogonal Dynamic Bonds in an Interpenetrating Network. *ACS Macro Lett.* **2017**, *6* (5), 495–499. https://doi.org/10.1021/acsmacrolett.7b00172.

(44) Zhang, B.; Watuthanthrige, N. D.; Wanasinghe, S. V.; Averick, S.; Konkolewicz, D. Complementary Dynamic Chemistries for Multifunctional Polymeric Materials. *Adv. Funct. Mater.* **2021**, *32* (8), 2108431. https://doi.org/10.1002/adfm.202108431.

(45) Mai, D.; Mo, J.; Shan, S.; Lin, Y.; Zhang, A. Self-Healing, Self-Adhesive Strain Sensors Made with Carbon Nanotubes/Polysiloxanes Based on Unsaturated Carboxyl–Amine Ionic Interactions. *ACS Appl. Mater. Interfaces* **2021**, *13* (41), 49266–49278. https://doi.org/10.1021/acsami.1c12438.

(46) Perrier, S. 50th Anniversary Perspective: RAFT Polymerization - A User Guide. *Macromolecules* **2017**, *50* (19), 7433–7447. https://doi.org/10.1021/acs.macromol.7b00767.

(47) Nguyen, G.; Nicole, D.; Matlengiewicz, M.; Roizard, D.; Henzel, N. Relation between Microstructure and Glass Transition Temperature of Poly[(Methyl Methacrylate)-Co-(Ethyl Acrylate)]. *Polym. Int.* **2001**, *50* (7), 784–791. https://doi.org/10.1002/pi.694.

(48) King, A. P.; Naidus, H. The Relationship between Emulsion Freeze-Thaw Stability and Polymer Glass Transition Temperature. I. A Study of the Polymers and Copolymers of Methyl Methacrylate and Ethyl Acrylate. *J. Polym. Sci. Part C Polym. Symp.* **1969**, *27* (1), 311–319. https://doi.org/10.1002/polc.5070270122.

(49) Van Steenberge, P. H. M.; D'Hooge, D. R.; Wang, Y.; Zhong, M.; Reyniers, M. F.; Konkolewicz, D.; Matyjaszewski, K.; Marin, G. B. Linear Gradient Quality of ATRP Copolymers. *Macromolecules* **2012**, *45* (21), 8519–8531.

https://doi.org/10.1021/ma3017597.

(50) SIGMA ALDRICH. 1,1′-(Methylenedi-4,1-phenylene)bismaleimide https://www.sigmaaldrich.com/specification-sheets/530/843/227463-BULK_____ALDRICH__.pdf (accessed Aug 29, 2022).

(51) Voorhaar, L.; Hoogenboom, R. Supramolecular Polymer Networks: Hydrogels and Bulk Materials. *Chem. Soc. Rev.* **2016**, *45* (14), 4013–4031. https://doi.org/10.1039/c6cs00130k.

(52) Feldman, K. E.; Kade, M. J.; Meijer, E. W.; Hawker, C. J.; Kramer, E. J. Model Transient Networks from Strongly Hydrogen-Bonded Polymers. *Macromolecules* **2009**, *42* (22), 9072–9081. https://doi.org/10.1021/ma901668w.

(53) Agnaou, R.; Capelot, M.; Tencé-Girault, S.; Tournilhac, F.; Leibler, L. Supramolecular Thermoplastic with 0.5 Pa·s Melt Viscosity. *J. Am. Chem. Soc.* **2014**, *136* (32), 11268–11271. https://doi.org/10.1021/ja505956z.

(54) Stubbs, C. J.; Khalfa, A. L.; Chiaradia, V.; Worch, J. C.; Dove, A. P. Intrinsically Re-Curable Photopolymers Containing Dynamic Thiol-Michael Bonds. *J. Am. Chem. Soc.* **2022**, *144* (26), 11729–11735. https://doi.org/10.1021/jacs.2c03525.

(55) Xiang, L.; Liu, X.; Zhang, H.; Zhao, N.; Zhang, K. Thermoresponsive Self-Healable and Recyclable Polymer Networks Based on a Dynamic Quinone Methide-Thiol Chemistry. *Polym. Chem.* **2020**, *11* (38), 6157–6162. https://doi.org/10.1039/d0py01008a.

(56) Zhang, B.; Digby, Z. A.; Flum, J. A.; Chakma, P.; Saul, J. M.; Sparks, J. L.; Konkolewicz, D. Dynamic Thiol-Michael Chemistry for Thermoresponsive Rehealable and Malleable Networks. *Macromolecules* **2016**, *49* (18), 6871–6878. https://doi.org/10.1021/acs.macromol.6b01061.

(57) Jiang, Z.; Bhaskaran, A.; Aitken, H. M.; Shackleford, I. C. G.; Connal, L. A. Using Synergistic Multiple Dynamic Bonds to Construct Polymers with Engineered Properties. *Macromol. Rapid Commun.* **2019**, *40* (10). https://doi.org/10.1002/marc.201900038.

(58) Zhang, B.; Digby, Z. A.; Flum, J. A.; Foster, E. M.; Sparks, J. L.; Konkolewicz, D. Self-Healing, Malleable and Creep Limiting Materials Using Both Supramolecular and

Reversible Covalent Linkages. *Polym. Chem.* **2015**, *6* (42), 7368–7372. https://doi.org/10.1039/c5py01214g.

(59) Shergold, O. A.; Fleck, N. A.; Radford, D. The Uniaxial Stress versus Strain Response of Pig Skin and Silicone Rubber at Low and High Strain Rates. *Int. J. Impact Eng.* **2006**, *32* (9), 1384–1402. https://doi.org/10.1016/j.ijimpeng.2004.11.010.

(60) Jin, Y.; Lei, Z.; Taynton, P.; Huang, S.; Zhang, W. Malleable and Recyclable Thermosets: The Next Generation of Plastics. *Matter* **2019**, *1* (6), 1456–1493. https://doi.org/10.1016/j.matt.2019.09.004.

(61) Hamerton, I.; Mooring, L. The Use of Thermosets in Aerospace Applications. *Thermosets* **2012**, 189–227. https://doi.org/10.1533/9780857097637.2.189.

(62) Chen, X.; Dam, M. A.; Ono, K.; Mal, A.; Shen, H.; Nutt, S. R.; Sheran, K.; Wudl, F. A Thermally Re-Mendable Cross-Linked Polymeric Material. *Science (80-.).* **2002**, *295* (5560), 1698–1702. https://doi.org/10.1126/science.1065879.

(63) Park, J. S.; Darlington, T.; Starr, A. F.; Takahashi, K.; Riendeau, J.; Thomas Hahn, H. Multiple Healing Effect of Thermally Activated Self-Healing Composites Based on Diels-Alder Reaction. *Compos. Sci. Technol.* **2010**, *70* (15), 2154–2159. https://doi.org/10.1016/j.compscitech.2010.08.017.

(64) Guo, Z.; Wang, W.; Liu, Z.; Xue, Y.; Zheng, H.; Majeed, K.; Zhang, B.; Zhou, F.; Zhang, Q. Preparation of Carbon Nanotube-Vitrimer Composites Based on Double Dynamic Covalent Bonds: Electrical Conductivity, Reprocessability, Degradability and Photo-Welding. *Polymer (Guildf).* **2021**, *235* (October), 124280. https://doi.org/10.1016/j.polymer.2021.124280.

(65) Self, J. L.; Reynolds, V. G.; Blankenship, J.; Mee, E.; Guo, J.; Albanese, K.; Xie, R.; Hawker, C. J.; de Alaniz, J. R.; Chabinyc, M. L.; Bates, C. M. Carbon Nanotube Composites with Bottlebrush Elastomers for Compliant Electrodes. *ACS Polym. Au* **2021**, acspolymersau.1c00034. https://doi.org/10.1021/acspolymersau.1c00034.

(66) Huang, S.; Liu, Y.; Zhao, Y.; Ren, Z.; Guo, C. F. Flexible Electronics: Stretchable Electrodes and Their Future. *Adv. Funct. Mater.* **2019**, *29* (6), 1–15.

https://doi.org/10.1002/adfm.201805924.

(67) Segev-bar, M.; Haick, H. Flexible Sensors Based on Nanoparticles. *ACS Nano* **2013**, *7* (10), 8366–8378. https://doi.org/10.1021/nn402728g.

(68) Ryu, D.; Loh, K. J.; Ireland, R.; Karimzada, M.; Yaghmaie, F.; Gusman, A. M. In Situ Reduction of Gold Nanoparticles in PDMS Matrices and Applications for Large Strain Sensing. *Smart Struct. Syst.* **2011**, *8* (5), 471–486. https://doi.org/10.12989/sss.2011.8.5.471.

(69) Thostenson, E. T.; Chou, T. W. Carbon Nanotube Networks: Sensing of Distributed Strain and Damage for Life Prediction and Self Healing. *Adv. Mater.* **2006**, *18* (21), 2837–2841. https://doi.org/10.1002/adma.200600977.

TABLE OF CONTENTS GRAPHIC